QRC-4-ESP

QUANTUM RESERVOIR COMPUTING
FOR EFFICIENT SIGNAL PROCESSING

Project Deliverable

D3.1 Report on point defect quantum systems in the presence of input-output signal, intrinsic decoherence & ambient noise

Lead beneficiary:	LIU
Author(s):	Son Nguyen
Contributor(s):	Danial Shafizadeh, Ivan Ivanov, and Igor Abrikosov
Date of issue:	12/12/2024
Dissemination level:	Public (PU)

https://www.qrc-4-esp.eu

Funded by
the European Union

DOCUMENT HISTORY

Version and date	Changes
1.0 - 12/12/2024	Initial version

DISCLAIMER

Funded by the European Union. Views and opinions expressed are however those of the author(s) only and do not necessarily reflect those of the European Union or the European Commission. Neither the European Union nor the granting authority can be held responsible for them.

Table of Contents

1. Introduction *4*

1.1 Scope of the Deliverable 4

1.2 Structure of the Deliverable 4

2. Choice of material platforms for point defect quantum systems *4*

3. Model of point defect quantum systems based on single Si vacancies in SiC *5*

3.1 The Si vacancy 5

3.2 Quantum system containing a small cluster of single Si vacancies 6

3.2.1 Spin-spin interactions and spin decoherence 7

3.2.2 Influence of local charge fluctuation on Si vacancy qubits 7

4. Mitigation of spin decoherence and ambient noise *7*

4.1 Pure SiC layers including isotope engineering 7

4.2 Stabilisation of Si vacancy emissions with minimal use of repump laser 7

5. Experimental investigations of point defect quantum systems in the presence of input-output signal, intrinsic decoherence & ambient noise *8*

5.1 Choices of samples 8

5.1.1 C-plane samples 8

5.1.2 A-plane samples 8

5.2 Adaptation and optimisation of a setup for PLE of single Si vacancies 8

5.3 Realisation of single vacancies and their small clusters 10

5.4 PLE measurements 12

6. Conclusions and outlook *13*

1. Introduction

Reservoir computing (RC) is an approach towards artificial intelligence (AI), where the input signal is mapped on the state of the reservoir (digital or analogue structure with a large space of states and nonlinear response). The reservoir state provides the input for a conventional neural network. The reservoir itself is not trained and can be realised by a wide class of different physical systems and devices, e.g., mechanical, electronic, mechatronic, photonic, etc, that satisfy a non-restrictive set of conditions. The nonlinear evolution of its state allows the use of simple training methods for the readout, which significantly speeds up training, decreases training costs and makes the approach especially convenient for real-time tasks.

Differing from conventional RC, quantum reservoir computing (QRC) is a fixed quantum system whose output is used to train a classical neural network. A quantum reservoir (QR) is a linear or nonlinear quantum system and has a massively greater space of states compared to a classical reservoir with the same number of unit elements. Moreover, a QR can accept quantum, rather than classical, inputs. This is critically important for the development of quantum sensing and imaging technologies.

Quantum reservoirs from several promising platforms, such as superconducting Josephson devices, semiconductor quantum dots, ion traps, neutral atoms, two-dimensional electron gas, and nuclear magnetic resonance (NMR), have been reported. While less mature, defect-based qubits in wide-bandgap semiconductors, including the NV centres in diamond or vacancies and divacancies in silicon carbide (SiC), have intrinsic advantages such as long spin coherence times, can operate in the optical range and at room temperature, and to be readily integrated with quantum devices.

In deliverable D3.1, we report our investigation and design of point defect quantum systems in SiC for developing QRs. The tasks are structured in Section 1.2 and presented in Sections 2 to 5.

1.1 Scope of the Deliverable

The present document provides detailed information on our design of point defect quantum systems based on defects in silicon carbide (SiC), description, and conducting experiments that determine their behaviour in a wide range of conditions for development of quantum reservoirs (QRs).

1.2 Structure of the Deliverable

The present Exploitation Plan is structured as follows:

1. Choice of material platforms for point defect quantum systems
2. Identification of point defect systems in SiC that can be used for QRs
3. Model of point defect quantum systems based on single Si vacancies in SiC
4. Mitigation of spin decoherence and ambient noise
5. Experimental investigations of point defect quantum systems in the presence of input-output signal, intrinsic decoherence & ambient noise.
   5.1. Choice of samples
   5.2. Adaptation and optimisation of a setup for photoluminescence excitation of single Si vacancies
   5.3. Realisation of single vacancies and their small clusters for QRs
   5.4 PLE measurements
6. Conclusions and outlook.

2. Choice of material platforms for point defect quantum systems

Optical defect-based qubits have been developed for several decades with the NV centre in diamond being the leading contender. Since the last decade, SiC has emerged as a promising platform since it hosts various

spin-active optical defects that can be realised bright single photon sources for optical spin qubits with long spin coherence times, which can be optically controlled even at room temperature. Among these, the Si vacancy and the divacancy show favourable optical and spin properties for quantum applications. Moreover, SiC is the only mature wide-bandgap semiconductor having industrial wafer scales, complementary metal oxide semiconductor (CMOS) compatible technology, and well-developed nanofabrication techniques. This is important for integration of qubits in quantum photonic devices, such as quantum cavities, resonators and waveguides, for enhancing their emissions, and in classical electronics, such as p-i-n diodes, for quantum sensing. Therefore, SiC is the material of choice for this project.

3. Model of point defect quantum systems based on single Si vacancies in SiC

Our research on QRC starts with intensive literature search for penetrating into this new research field. We find that most of the reported studies are concerning theoretical simulations of QRs. Experimental works are very rare with QRs limited to a system with two quantum states, e.g., a single trapped ion [1]. To the best of our knowledge, no experimental work on QRs based on point defects in semiconductors has been reported so far.

Our task is to develop a quantum system containing a number of qubits, which should satisfy the requirements for a QR, i.e., its qubits nonlinearly interact with each other and their states, either without or under external perturbations, can be monitored and registered. Our interest is in the electron spins associated with optical point defects but not nuclear spins since the spin-spin interaction between nuclei is nearly 2000 times weaker.

Among the intrinsic point defects, the negative Si vacancy (V_{Si}^-) formed by a missing Si atom at a lattice site with captured one extra electron, and the neutral divacancy ($V_CV_{Si}^0$), i.e., an uncharged complex consisting of a C vacancy (VC) and a nearest-neighbour Si vacancy, are the most studied ones with their qubit performance approaching the level of the NV centre in diamond. The realisation of single defects is well-controlled for the Si vacancy and divacancy. However, compared to the Si vacancy, the divacancy has more complicated excited state 3E, which contains six levels with the two lowest lying ones being unresolved. Also, creation of divacancies requires high-temperature annealing (~750-800 °C), which leads to the formation of other unwanted vacancy-related complexes such as the C antisite-vacancy $C_{Si}V_C$ and N_CV_{Si} complexes. Therefore, we choose to develop and study quantum systems based on single Si vacancies.

3.1 The Si vacancy

In 4H-SiC, the Si vacancy at the two inequivalent hexagonal (h) and quasi-cubic (k) lattice sites, labelled as V_{Si}(h) and V_{Si}(k) (Fig. 1a), has axial symmetry. In the negative charge state, the vacancy centres V_{Si}^-(h) and V_{Si}^-(k) (labelled as V1 and V2, respectively) give rise to two photoluminescence (PL) emissions with the zero-phonon line (ZPL) at 861 nm (for V1) and 917 nm (for V2). Their PL and ODMR can be detected at room temperature and their zero-field splitting (ZFS) D values are temperature independent in the range 4-300 K.
The negative Si vacancy in SiC has three unpaired electrons and, hence, an electron spin 3/2. Schematic energy level diagram of V_{Si}^- is shown in Fig. 1b. The ZFS of the ground state (GS) $2D_{GS}$ is 10 MHz for V1 and 70 MHz for V2. The corresponding ZFS for the excited state (ES) is 985 MHz for V1 and 1 GHz for V2. The spin-conserving transitions A_1 and A_2 give rise to ZPLs, which are not resolved in conventional PL measurements due to their small separation of just 1 GHz. However, in the photoluminescence excitation (PLE) spectrum using lasers with linewidths in the range of tens of kHz, the A_1 and A_2 ZPLs are well-resolved.

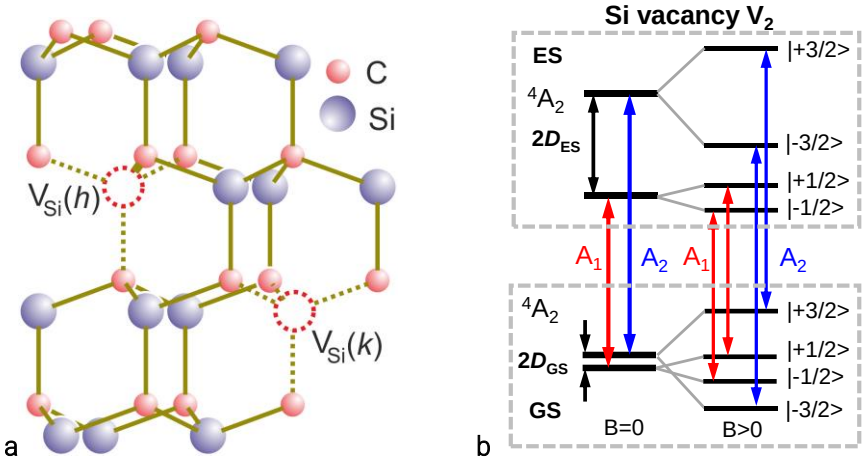

Fig.1. **a** Two Si vacancy configurations V1 and V2 in 4H-SiC. **b** Energy level diagram of the V2 centre. The diagram for V1 is similar but with different zero-field splitting (ZFS). Ground (GS) and excited (ES) states are spin-quartets and optical transitions are spin conserving denoted A_1 and A_2. The ZFS of the GS is $2D_{GS}$ = 70 MHz. The separation between A_1 and A_2 lines is the $2D_{ES} - 2D_{GS}$, which is 1 GHz.

3.2 Quantum system containing a small cluster of single Si vacancies

We consider quantum system of several single Si vacancies containing several single emitters within the spot of the excitation laser, whose typical size is ~1 μm^2 (Fig. 2). For single defect studies, the density of single Si vacancies needs to be one in a laser spot, i.e., their concentration must be in the range of ~10^{12} cm^{-3}. For a quantum system containing a few single vacancies within a laser spot, the density should be a few times higher or ~10^{13} cm^{-3}.

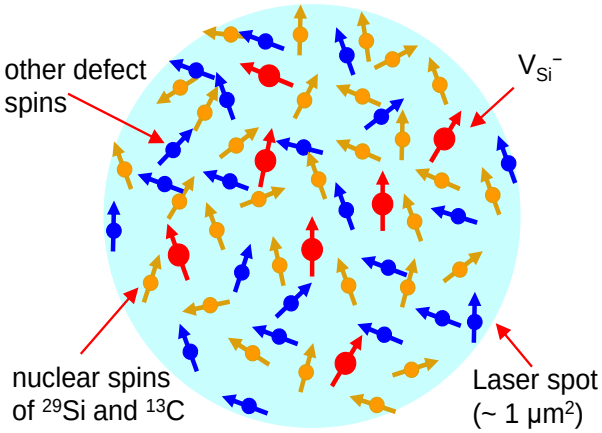

Fig. 2. A small quantum system containing several single Si vacancies within the laser spot (~1 μm^2). The system is embedded among other defect spins and nuclear spins of ^{13}C and ^{29}Si nuclei.

The dominant residual impurity in SiC is the N donor (electron spin S = 1/2), while dominant intrinsic defect in pure SiC is the C vacancy. In addition, natural SiC contains two host-atom isotopes with nonzero nuclear spins, which are ^{13}C (nuclear spin I = 1/2, 1.1% natural abundance) and ^{29}Si (I = 1/2, 4.7%). In commercial SiC layers grown by chemical vapour deposition (CVD), the typical concentration of the residual impurities is in the range of mid-10^{14} to low-10^{15} cm^{-3} for the N donor. The C vacancy is the dominant intrinsic defect in CVD layers and has a typical density in the 10^{14} cm^{-3} range.

The idea of a quantum system containing a small cluster of Si vacancies was suggested at the kick-off Loughborough Workshop in February 2024. Since then, the model and its possible inputs and outputs have been discussed at our weekly meeting on Thursday. Another quantum system, such as a single Si vacancies coupled to five neighbouring nuclear spins, was also suggested. It was intensively discussed during weekly theoretical meetings and, especially at the workshop in Montpellier in September 2024. Finally, we abandoned this system for several reasons: (i) the interaction between nuclear spins with very weak

magnetic moment (nearly 2000 times weaker than that of electron) is negligible because magnetic interaction is a short-range interaction, (ii) the hyperfine interaction between electron spin and nuclear spins is independent of the magnetic field and the excitation of photons (such as light, radio frequency (RF), or microwave frequency (MW)), and does not vary with time, and (iii) it is not possible to distinguish the contributions of individual nuclei to the overlapping hyperfine signals.

3.2.1 Spin-spin interactions and spin decoherence

The dipole interactions of Si vacancies with each other, with electron spins of residual impurities and intrinsic defects, and with nuclear spins of ^{13}C and ^{29}Si nuclei in the lattice are the main source of magnetic noises that cause the decoherence of Si vacancy qubits. However, the magnetic interaction is a short-range interaction, which is limited to distances below 20 nm. Therefore, the dipole interaction is local and limited to defects located very close to the Si vacancy qubit. Also, not all the impurities and defects are in spin-active charge states, e.g., the C vacancies are mostly in the double negative charge state and only part of them are ionised by optical excitation into single negative charge state with spin S = 1 but will quickly relax to the negative-U, double negative state with spin zero by capturing an electron again. The ionised N donors have no electron spin. The low natural abundance of ^{13}C and ^{29}Si isotopes is low and, hence, the influence of the nuclear spin bath is not so severe. Therefore, in commercial SiC materials, the spin coherence time can reach a few hundreds of µs, which should be enough for applications in QRs.

3.2.2 Influence of local charge fluctuation on Si vacancy qubits

Under optical excitation, defects can be ionised and change their charge states. This induces charge fluctuations surrounding Si vacancy qubits and, hence, the local electric field. This causes changes in the fine structure of the excited states of Si vacancy qubits and their optical transitions, resulting in random jumps in the energy of the zero-phonon line (ZPL). While small jumps in energy induce inhomogeneous broadening of the optical linewidths, larger jumps can shift the energy of the ZPL in the range of several GHz as reported for a small cluster of single Si vacancies [2]. The intensity and linewidth of single Si vacancies are also sensitive to the power of the excitation laser.

With increasing the density of single emitters to a level that a few of such individual Si vacancies are present in a laser spot, we can have a quantum systems containing a small cluster of single V_{Si} centres as illustrated in Fig. 2. The variation in the ZPL energy, linewidth, and intensity of individual Si vacancies of such a quantum system can be constantly monitored and registered in PLE scans.

4. Mitigation of spin decoherence and ambient noise

4.1 Pure SiC layers including isotope engineering

A straight way to mitigate the spin decoherence and electric noise is to reduce the concentration of residual impurities and intrinsic defects in the material. We use pure 4H-SiC layers with the concentration of N down to mid-10^{13} cm^{-3} and the density of the C vacancy is in the range from 5×10^{12} to low 10^{13} cm^{-3}. We also develop CVD processes for growing isotopically enriched 4H-$^{28}Si^{12}C$ layers with 99.85 % of ^{28}Si and 99.98% of ^{12}C for reducing the magnetic noise from the nuclear spin bath. In such isotope-purified materials, spin coherence times T_2 in the millisecond ranges can be achieved. In our pure SiC layers, inhomogeneous broadening of optical linewidths is shown to be greatly reduced and for many single Si vacancies, the linewidth approaches the lifetime-limited linewidth.

4.2 Stabilisation of Si vacancy emissions with minimal use of repump laser

During optical excitation, defects can be ionised and change their charge state. This can also happen to single Si vacancies and change them from bright to dark state, resulting in bleaching of PL emissions. For stabilisation the charge state of Si vacancy centres, a repump laser with higher photon energy is used for recovering the bright charge state and stabilising of the emission. However, repump laser also enhances the ionisation processes and, hence, triggers unwanted charge fluctuations. Fortunately, PLE experiments use resonant excitation with low powers and the defect ionisation is not pronounce. In our materials, the charge state of single Si vacancies is stable for a long period, and we could run 100 PLE scans without using repump

laser as shown in Fig. 3.

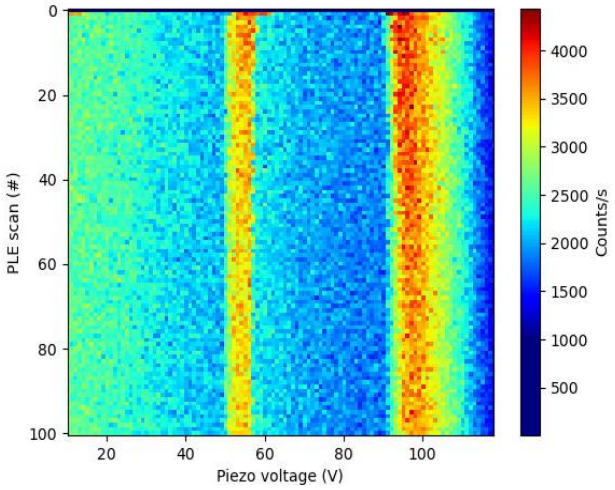

Fig. 3. Map of 100 PLE scans of a Si vacancy V2 centre collected under resonant excitation (1 μW) without repump laser showing stable emission. The bright parts correspond to the peak position of the ZPLs A_1 and A_2. Due to temporary lack of Fabry-Pérot interferometer for frequency determination, the x-axis is the piezo voltage.

5. Experimental investigations of point defect quantum systems in the presence of input-output signal, intrinsic decoherence & ambient noise

5.1 Choices of samples

The PL emission of the V1 and V2 Si vacancy centres can only be detected in the direction perpendicular to the c-axis of the hexagonal SiC lattice, while only c-plane wafers are commercially available. The PL detection in c-plane samples requires detection from the edge. The natural SiC samples are used for optimization of the cluster, while isotope-pure samples are needed for reducing the influence of the nuclear spin bath.

5.1.1 C-plane samples

For the usual C-plane samples, we cleave their edges instead of cutting to obtain optical accessible edge for detection of PL emissions from the edge. This is a common way for detection of Si vacancy emissions. Most of our samples are c-plane samples. However, the cleaved edge of the sample is usually not flat that making it more difficult to detect PL, PLE, and ODMR signals.

5.1.2 A-plane samples

A-plane SiC substrates, i.e., wafers have been cut with the surface in the (11-20) plane. In these samples, the PL emission of V_{Si} centres can be conveniently detected from the surface. We have a few pieces of a-plane 4H-SiC substrates and could grow some CVD layers including an isotope-purified layer. These samples are needed for detection of emissions from the Si vacancy from perpendicular to the c-direction.

A list of all types of samples with their specifications and the fluences of electrons are given in Table 1

5.2 Adaptation and optimisation of a setup for PLE of single Si vacancies

Figure 4a provides an overview of our optical laboratory. The setup is a home-built confocal microscopy for photoluminescence (PL) and optically detected magnetic resonance (ODMR) of ensemble and single emitters in the spectral range from visible to telecom wavelengths (400-1700 nm) using two APD detectors (400 – 920 nm) or a two-channel superconducting nanowire photon counting detector (optimised in the

range of 1300 -1550 nm). The sample temperature can be regulated from 3.5 K to room temperature using a closed-cycle cryostat Montana S50. Since there is no option of a magnet for this type of cryostat, we built ourselves a magnet as shown in Fig. 4b (two coils around the cryostat) for ODMR experiments.

For PLE of the Si vacancy (near 861 nm and 917 nm, for V1 and V2, respectively), we need a new set of tuneable Toptica lasers. When our suggestion of a quantum system containing a small cluster of single Si

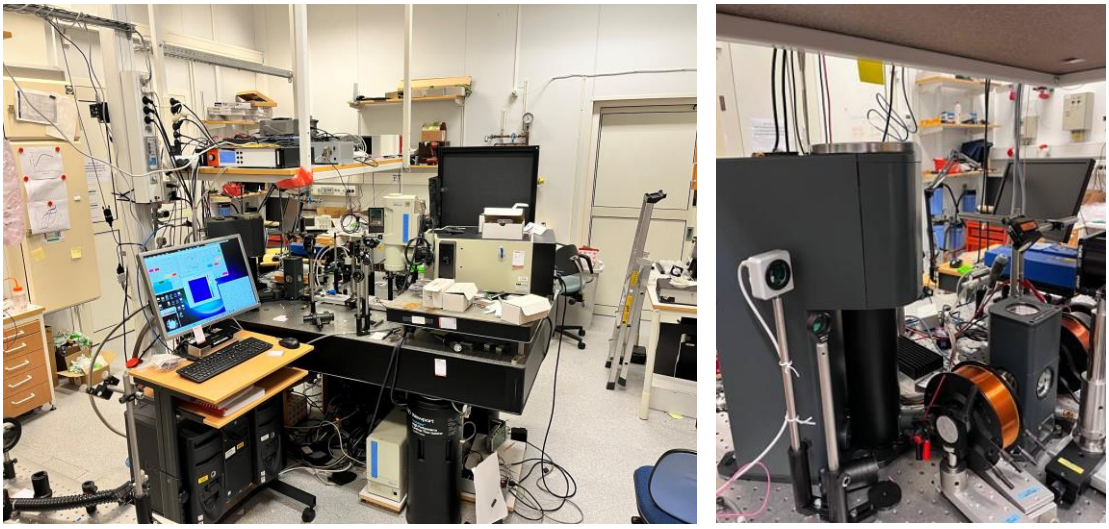

a **b**

Fig. 4. a An overview of the confocal PL and ODMR setup. **b** The setup is equipped with a close-cycled cryostat (Montana S50) and a home-built magnet.

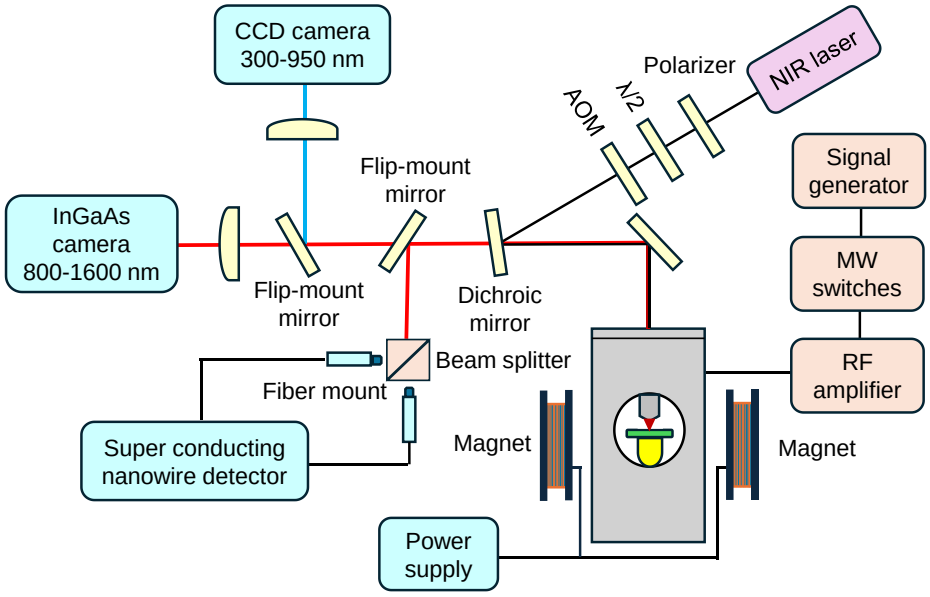

Fig. 5. Sketch of the optical setup for the ODMR and PLE experiments.

vacancies for QRs received theoretical support from other partners in the consortium after many discussions at the workshop in Loughborough 29 January – 02 February 2024, and on weekly Thursday theory seminars, we decided to order new Toptica lasers covering the spectral range of the Si vacancies. The lasers were ordered on February 15 but delivered only in August 2024, and we started building PLE setup for the spectral region 850-920 nm. The sketch of the PLE setup is shown in Fig. 5. Unfortunately, the delivery of the Fabry-Pérot interferometer needed for determination of wavelengths is delayed until January 2025. This causes

several problems. Firstly, it is difficult to tune the laser in resonantly with the energy of the ZPL. Secondly mode hops leading to uncontrolled wavelength jumps cannot be eliminated and the wavelength of the laser is not accurately known. Now we try to solve the first problem by blindly rough-tuning and fine-scanning the laser wavelength until we observe the signal, and then work with this empirically found but not accurately known range for the scan. Thus, we are unable to know exactly the frequency in the PLE spectra but only the voltage applied to the piezo. When we get the Fabry-Pérot interferometer, the frequency of the laser will be determined exactly.

5.3 Realisation of single vacancies and their small clusters

We create Si vacancies by 2 MeV-electron irradiations at room temperature. With this high energy, vacancies are created homogeneously within the whole sample. We already know that the electron fluence needed for creation of single Si vacancies at the concentration suited for single emitter studies is 1×10^{12} cm^{-2}. For finding a suitable fluence of electrons for creation of Si vacancy clusters, we perform electron irradiations with different fluences ranging from 5×10^{12} to 5×10^{14} cm^{-2}. We have irradiated 15 samples (Fig. 5), and their specifications are given in Table 1. Confocal scans have been performed on all samples. Fig. 6a shows a confocal fluorescence image scanned in a sample irradiated with the electron fluence of 1×10^{12} cm^{-2} and Fig. 6b shows a confocal fluorescence image scanned in a 4H-SiC sample irradiated with an electron fluence of 1×10^{14} cm^{-2}. We do not count the number of emitters for estimation of their density since there can be some emitters belonging to other defects and not relate to the Si vacancy. We check ODMR of some bright spots to verify if it gives a resonant at 70 MHz specific for the Si vacancy V2 centre (Fig. 7) and then test PLE to see how many single vacancies are involved in that spot. Based on our available data on the dependence of the concentration of the Si vacancy V2 centre on the electron fluence, we estimate the concentration of the Si vacancies.

Table 1. List of 4H-SiC samples irradiated with 2 MeV electrons. same samples from natural SiC and isotope -pure $^{28}Si^{12}C$ series were irradiated with the same electron fluence of 1×10^{14} cm^{-2}, one of which is annealed to form the divacancy. After checking the Si vacancies, some samples were annealed at 750 ℃ for study of the divacancy.

Samples	Sample type	Thickness (μm)	N concentration (cm^{-3})	Electron fluence (cm^{-2})	Isotope-purified $^{28}Si^{12}C$
X771-01	c-plane	~100	1×10^{13}	5×10^{12}	No
X771-02	c-plane	~100	1×10^{13}	1×10^{13}	No
X771-03	c-plane	~100	1×10^{13}	6×10^{13}	No
X771-04	c-plane	~100	1×10^{13}	1×10^{14}	No
X771-05	c-plane	~100	1×10^{13}	1×10^{14}	No
X771-06	c-plane	~100	1×10^{13}	5×10^{14}	No
HL1032-01	c-plane	~110	6×10^{13}	5×10^{12}	Yes
HL1032-02	c-plane	~110	6×10^{13}	1×10^{13}	Yes
HL1032-03	c-plane	~110	6×10^{13}	5×10^{13}	Yes
HL1032-04	c-plane	~110	6×10^{13}	5×10^{13}	Yes
HL1032-05	c-plane	~110	6×10^{13}	1×10^{14}	Yes
HL1032-06	c-plane	~110	6×10^{13}	1×10^{14}	Yes
HL1028-01	a-plane	~25	3×10^{15}	1×10^{13}	Yes
HL1028-02	a-plane	~25	3×10^{15}	5×10^{13}	Yes
HL1028-03	a-plane	~25	3×10^{15}	1×10^{14}	Yes

Fig. 5. Three series of 4H-SiC layers (15 samples) that irradiated by 2MeV-electrons with different fluences from 5×10^{12} to 5×10^{14} cm^{-2} at room temperature.

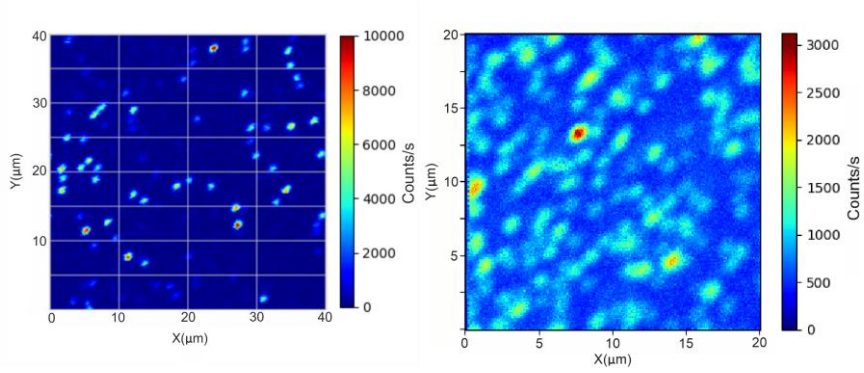

Fig. 7. **a** Confocal fluorescence image in a 4H-SiC samples irradiated by electrons with a fluence of **a,** 1×10^{12} cm^{-2} when most of the emitters are single Si vacancies. **b,** 1×10^{14} cm^{-2} when most of the emitters consist of a few Si vacancies. The laser excitation wavelength is 890 nm. The larger sizes of emitters in **b** partly due to it's a zoomed map (by a factor of two).

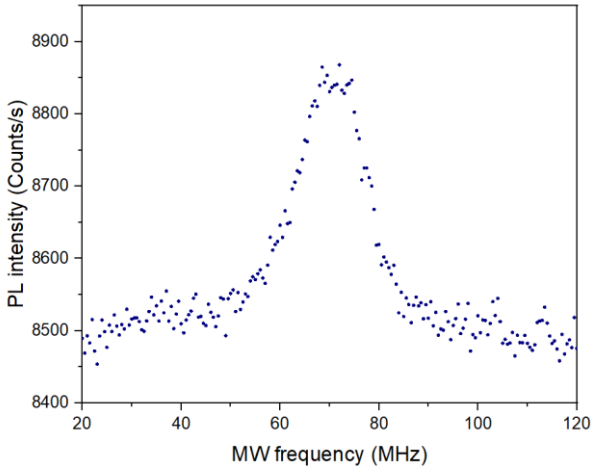

Fig. 7. ODMR spectrum measured on an emitter in a 4H-SiC sample irradiated to 5×10^{13} cm^{-2}. The observation of the ODMR signal at 70 MHz confirms that the emitter is from the Si vacancy V2 centre.

5.4 PLE measurements

Our chosen quantum system contains several single Si vacancies within a laser spot as described in Section 3.2. The response of the system will be monitored and registered by PLE measurements. The Sketch of the optical setup for PLE experiments is shown in Fig. 5. Fig. 8 shows PLE spectra observed in different spots consisting of different in size clusters of Si vacancies. Fig. 9 shows a PLE maps containing of 100 PLE scans taken continuously one after other. Due to charge fluctuation (i.e., fluctuation of the electric field) in the local environment, the energy of the ZPLs is randomly shifting between the scans as can be seen in the figure.

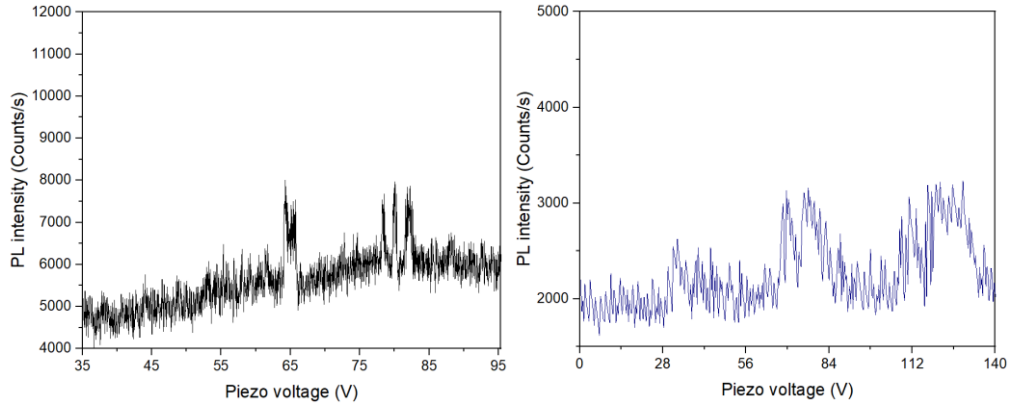

Fig. 8. PLE spectra measured in a sample irradiated to the electron fluence of 5×10^{13} cm^{-2} from spots consisting of (a) a few Si vacancies and (b) a larger cluster of Si vacancies.

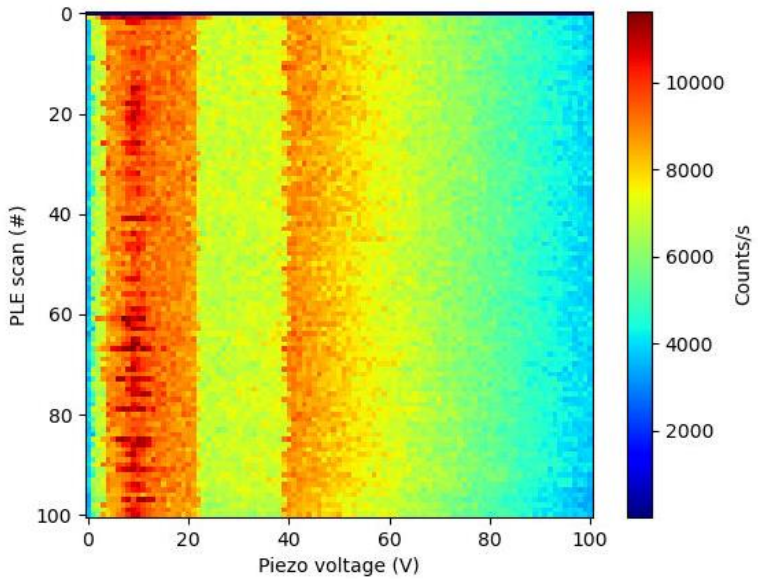

Fig. 9. A map of 100 PLE spectra measured on a spot in a sample irradiated to the electron fluence of 5×10^{13} cm^{-2}. The red parts correspond to the position of the ZPL constituents A_1 and A_2. It is apparent that the peak positions and the peak intensities change between the scans because of the random fluctuation of local charges.

6. Conclusions and outlook

From the PLE spectrum, the following parameters of Si vacancy qubits for A_1 and A_2 ZPLs corresponding to transitions between |±1/2> ↔ |±1/2> and between |±3/2> ↔ |±3/2>, respectively, as shown in Fig. 1b, can be extracted.

- The energy (frequency) of A_1 and A_2 ZPLs
- The linewidth of A_1 and A_2 ZPLs
- The intensity of A_1 and A_2 ZPLs

We conclude that it is possible to change the conditions of PLE measurements, e.g., under

- Different laser powers
- External magnetic field that splits off the Zeeman levels |±1/2> and |±3/2> in the GS and ES states as shown in Fig. 1b.
- Application of microwave (MW) or radio frequency (RF) waves resonantly with Zeeman splitting levels to induce changes in the population on related levels (Fig. 1b).

Thus, the laser power, the frequency and the power of the MW (under external magnetic field) form a set of input data, while parameters, such as the energies, linewidths and intensities of A_1 and A_2 ZPLs, are output data of the quantum system.

In summary, we conclude that by repeating PLE measurements with variation of inputs, series of output data can be obtained. Achieving results for Deliverable 3.1 in our on experiments point defect quantum systems in the presence of input-output signal, intrinsic decoherence & ambient noise, as specified above, we have built a firm ground for the continuation of the project. In the next project period, will study optimal point defect ensembles in SiC and input-output methods for the QR. We will further improve our capabilities with equipment for determination of the wavelength of the laser. Receiving the Fabro-Pérot interferometer in January 2025, we will know exact frequency (or wavelength) of the laser.

References

[1] D. Kienzler, H.-Y. Lo, B. Keitch, L. de Clercq, F. Leupold, F. Lindenfelser, M. Marinelli, V. Negnevitsky, J. P. Home, Science 347, 53 (2015).

[2] R. Nagy, D. B. R. Dasari, C. Babin, D. Liu, V. Vorobyov, M. Niethammer, M. Widmann, T. Linkewitz, I. Gediz, R. Stöhr, H.B. Weber, T. Ohshima, M. Ghezellou, N. T. Son, J. Ul-Hassan, F. Kaiser, Jörg Wrachtrup, App. Phys. Lett. 118, 144003 (2021).